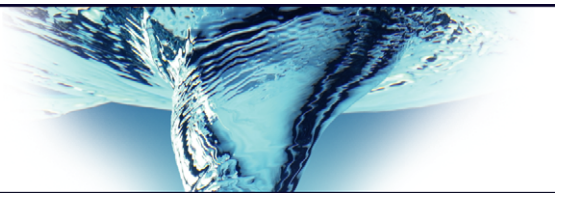
J. Fluid Mech. (2013), *vol.* 734, R4, doi:10.1017/jfm.2013.504



JFM RAPIDS
journals.cambridge.org/rapids

The two classes of primary modal instability in laminar separation bubbles

Daniel Rodríguez[1,2,†], Elmer M. Gennaro[2] and Matthew P. Juniper[3]

[1]School of Aeronautics, Universidad Politécnica de Madrid, Pza. Cardenal Cisneros 3, E-28040 Madrid, Spain

[2]Department of Aeronautics, São Carlos School of Engineering, Universidade de São Paulo, Rua Jõao Dagnone 1100, 13563-120, São Carlos, Brazil

[3]Department of Engineering, University of Cambridge, Trumpington Street, Cambridge CB2 1PZ, UK

(Received 1 August 2013; revised 18 September 2013; accepted 20 September 2013; first published online 10 October 2013)

The self-excited global instability mechanisms existing in flat-plate laminar separation bubbles are studied here, in order to shed light on the causes of unsteadiness and three-dimensionality of unforced, nominally two-dimensional separated flows. The presence of two known linear global mechanisms, namely an oscillator behaviour driven by local regions of absolute inflectional instability and a centrifugal instability giving rise to a steady three-dimensionalization of the bubble, is studied in a series of model separation bubbles. These results indicate that absolute instability, and consequently a global oscillator behaviour, does not exist for two-dimensional bubbles with a peak reversed-flow velocity below 12 % of the free-stream velocity. However, the three-dimensional instability becomes active for recirculation levels as low as $u_{rev} \approx 7\,\%$. These findings suggest a route to the three-dimensionality and unsteadiness observed in experiments and simulations substantially different from that usually found in the literature of laminar separation bubbles, in which two-dimensional vortex shedding is followed by three-dimensionalization.

Key words: absolute/convective instability, boundary layer instability, boundary layer separation

1. Introduction

Flow separation is invariably associated with adverse effects on the performance of lifting surfaces, which has motivated research efforts spanning more than half a century. However, despite continuous research, many questions concerning the appearance, structure and behaviour of separation bubbles remain open. Some of these

† Email address for correspondence: dani@torroja.dmt.upm.es

© Cambridge University Press 2013

https://doi.org/10.1017/jfm.2013.504 Published online by Cambridge University Press

questions are related to the laminar separation bubble (LSB) formed on the leading edge of thin aerofoils as the angle of attack is increased at near-stall conditions. These bubbles are classified as short or long according to their extent over the streamwise direction and have distinctly different impacts on the aerodynamic properties of the aerofoil (Gault 1949; McCullough & Gault 1951). The process through which a short bubble suddenly fails to reattach and becomes a long bubble after a small variation in angle of attack or Reynolds number is referred to as bursting. Its physical causes and the determination of an adequate criterion for predicting its occurrence are still today an active topic of research (Gaster 1967; Pauley, Moin & Reynolds 1990; Diwan, Chetan & Ramesh 2006; Marxen & Henningson 2011).

The usual picture of LSBs considers the inviscid instability of the separated shear layer to lead to laminar–turbulent transition, and turbulent mixing to be ultimately responsible for the reattachment of the flow. This picture suggests considering the local properties of the boundary layer at separation as a criterion for bursting. Besides bursting, the prediction of other characteristics of separated flow such as the onset of unsteadiness or three-dimensionalization of nominally two-dimensional LSBs has been attempted following this vein. The presence and dominance of Kelvin–Helmholtz (K–H) instability acting on the shear layer has been confirmed in a multitude of experimental (Dovgal, Kozlov & Michalke 1994) and numerical (Gruber, Bestek & Fasel 1987; Rist & Maucher 1994; Marxen, Lang & Rist 2012) investigations. External instability waves reaching the separated region experience a growth of several orders of magnitude, eventually leading to nonlinear effects and vortex shedding unless the initial amplitudes are very small. This description of LSBs as amplifiers of external perturbations does not suffice, however, to explain the onset of unsteadiness observed in direct numerical simulations (DNS) of unperturbed separated flow, nor the occurrence of flapping (Zaman, McKinzie & Rumsey 1989). Absolute/convective instability analysis (Huerre & Monkewitz 1990) suggests that, besides the amplifier character of the bubbles, they can also act as oscillators when a spatial region of the underlying base state sustains instability waves that propagate upstream. A global oscillator instability mechanism would exist in this case, intrinsic to the bubble and independent of external excitations, that ultimately would result in vortex shedding. Some theoretical studies were conducted in the past addressing this possibility (Allen & Riley 1995; Hammond & Redekopp 1998), and some researchers (e.g. Pauley *et al.* 1990) even suggested bursting to be directly related to the onset of absolute instability, but there is no general consensus on this point (Diwan & Ramesh 2009; Marxen & Henningson 2011).

The view of separated flow instability as a phenomenon associated with weakly non-parallel inflectional profiles led to the use of locally parallel linear stability for the study of instability waves. While this approach has been shown to be adequate even for realistic, non-parallel LSBs (Rist & Maucher 2002; Diwan & Ramesh 2012), it precludes the discovery and characterization of other mechanisms of instability. Marxen *et al.* (2012) survey the different local linear mechanisms, illustrating the ability of LSBs to amplify a wide range of externally imposed disturbances, but no new intrinsic mechanism was discovered that explains the onset of unsteadiness or three-dimensionality in unforced bubbles.

On the other hand, in the last decade there has been increased activity in global (or BiGlobal) instability analysis without resorting to locally parallel flow approximations, following the advances in computational capabilities necessary to support the associated numerical work (Theofilis 2003, 2011). Following this approach, the stability of a two-dimensional base state is studied by means of partial-derivative-

https://doi.org/10.1017/jfm.2013.504 Published online by Cambridge University Press

based eigenvalue problems. This analysis encompasses (as shown by e.g. Juniper, Tammisola & Lundell 2011) but is not restricted to wave-like disturbances, and three-dimensional modal perturbations of arbitrary shape are considered, thus enabling the discovery of global mechanisms different from the K–H instability. Worthy of mention is the work of Dallmann & Schewe (1987), in which they postulate the existence of a global mechanism acting on nominally two-dimensional separation bubbles that would cause a three-dimensionalization of the flow, eventually leading to unsteadiness. They regret the absence, at that time, of an analysis methodology able to address this kind of instability. It was not until the work of Theofilis, Hein & Dallmann (2000) that the required global stability analysis was applied to a separation bubble on a flat plate, demonstrating the existence of the self-excited three-dimensional instability mode. Similar results have been reported for geometries comprising two-dimensional recirculation regions (Barkley, Gomes & Henderson 2002; Gallaire, Marquillie & Ehrenstein 2007; Marquet *et al.* 2008; Kitsios *et al.* 2009), and the global eigenmode was shown to be connected to a centrifugal instability. Studies of the topological changes caused by the three-dimensional instability both on flat-plate LSBs (Rodríguez & Theofilis 2010*b*) and on a stalled NACA 0015 aerofoil (Rodríguez & Theofilis 2010*a*) (representative of a trailing-edge bubble) related these three-dimensional global instability modes to the cellular separation patterns, or 'stall cells', that have been observed experimentally at high Reynolds numbers (cf. Yon & Katz 1998 and references therein).

A question that remains open is the ability to predict the onset of global instability (either the global oscillator or the centrifugal instability) in separated flow on the basis of base or mean flow measurements and a simple criterion. In this respect, the ratio between the peak value of the reversed flow and the free-stream velocity $u_{rev} = u^*_{rev}/U^*_\infty$ (the non-dimensionalization used is described in § 2) was proposed to define the onset of absolute instability in the shear-layer profile (Huerre & Monkewitz 1985). Analyses of shear-layer profiles in the presence of a wall (Allen & Riley 1995; Hammond & Redekopp 1998; Rist & Maucher 2002; Diwan 2009), a geometry representative of LSBs, agree on a value $u_{rev} \approx 17$–$25\,\%$ for the onset of absolute instability, in line with results from DNS (Alam & Sandham 2000; Fasel & Postl 2004). Conversely, unsteadiness and vortex shedding have been reported consistently in unforced three-dimensional simulations in which the peak reversed flow of the mean flow was as low as $u_{rev} \approx 7$–$10\,\%$. Scenarios of global instability have been postulated (Dallmann & Schewe 1987; Watmuff 1999; Theofilis *et al.* 2000; Gaster 2004) to explain the origin of unsteadiness, but the unequivocal identification of such global instability mechanisms and the associated criteria is still lacking.

The present study revisits the global instability of nominally two-dimensional LSBs on a flat-plate with the aim of ascertaining which of the two potentially self-excited mechanisms described above is dominant and serves as the triggering mechanism towards three-dimensional unsteady states in the absence of external disturbances. Section 2 describes a non-similar formulation of the boundary-layer equations that is employed in order to generate a set of base LSBs. In choosing the current formulation, the possibility of the appearance of bubble shedding as the peak reversed flow increases is circumvented in the computation of the base flow and may be subsequently recovered as a global instability of the flow. Section 3 studies the global oscillator behaviour by means of a locally parallel analysis analogous to that of Hammond & Redekopp (1998), while § 4 is devoted to the three-dimensional centrifugal instability. The conclusions and implications of the results are discussed in § 5.

https://doi.org/10.1017/jfm.2013.504 Published online by Cambridge University Press

2. Base flow construction

A non-similar inverse formulation of the boundary-layer equations on a flat plate is used to obtain the base flows. The computed base separation bubbles are two-dimensional and steady by construction, and consequently the three-dimensionalization and/or occurrence of vortex shedding, in the cases in which they appear, is recovered as instabilities of this base flow.

2.1. *Inverse formulation of the non-similar boundary-layer problem*

The physical dimensional streamwise x^* and wall-normal y^* coordinates, an arbitrary characteristic length in the streamwise direction L^*, the boundary-layer edge velocity U_e^*, and the kinematic viscosity ν^* are used to define the non-dimensional boundary-layer variables $\xi = x^*/L^*$ and $\eta = y^*\sqrt{U_\infty^*/\ \nu^* x^*}$ and a transformed stream function

$$f(\xi, \eta) = \Psi/\sqrt{U_e^* \nu^* x^*}. \tag{2.1}$$

On introducing these variables into the streamwise momentum equation, an equation for the transformed stream function $f(\xi, \eta)$ is obtained. In order to recover separated states, the Reyhner and Flügge–Lotz (FLARE) approximation (Cebeci & Cousteix 2005) is invoked, which neglects the streamwise convective term when reversed flow exists. The boundary-layer equation is written as

$$f_{\eta\eta\eta} + \frac{m+1}{2} f f_{\eta\eta} + m\left(1 - f_\eta^2\right) = \xi\left(\theta f_\eta f_{\xi\eta} + f_{\eta\eta} f_\xi\right), \tag{2.2}$$

where subscripts imply partial differentiation, and $m = (\xi/U_e^*)(\mathrm{d}U_e^*/\mathrm{d}\xi)$ is the deceleration parameter, which depends on ξ. The FLARE approximation appears in this equation as the function θ, which takes value unity when $f_\eta \geqslant 0$ and vanishes if $f_\eta < 0$. This problem is solved subject to the boundary conditions

$$f(\xi, 0) = 0, \quad f_\eta(\xi, 0) = 0 \quad \text{and} \quad f_\eta(\xi, \eta \to \infty) \to 1. \tag{2.3}$$

To avoid Goldstein's singularity, which would appear at the separation point if an $m(\xi)$ distribution were imposed, the displacement thickness measured in the transformed variable η is imposed here as an asymptotic boundary condition:

$$f(\xi, \eta \to \infty) \to 1 - \bar{\delta}(\xi). \tag{2.4}$$

The solution algorithm iterates on each ξ profile until a converged solution profile $f(\xi, \eta)$ and $m(\xi)$ is obtained. Further details on the solution procedure can be found in Rodríguez & Theofilis (2010*b*).

2.2. *The boundary-layer-based LSB model base flows*

The two-dimensional LSB base states are constructed using the calculated transformed stream function $f(\xi, \eta)$. The streamwise and wall-normal dimensional velocity components are obtained using the transformation:

$$u^* = U_e^* f_\eta, \quad v^* = \frac{1}{2}\sqrt{\frac{U_e^* \nu}{\xi}}\left[f(m+1) + 2\xi f_\xi + \eta f_\eta (m-1)\right]. \tag{2.5}$$

In what follows, lengths are scaled using the dimensional displacement thickness at the inflow boundary, δ_{in}^*, and velocities are scaled with the inflow far-field velocity, U_∞^*. The non-dimensional spatial variables are denoted by x and y and the base flow

https://doi.org/10.1017/jfm.2013.504 Published online by Cambridge University Press

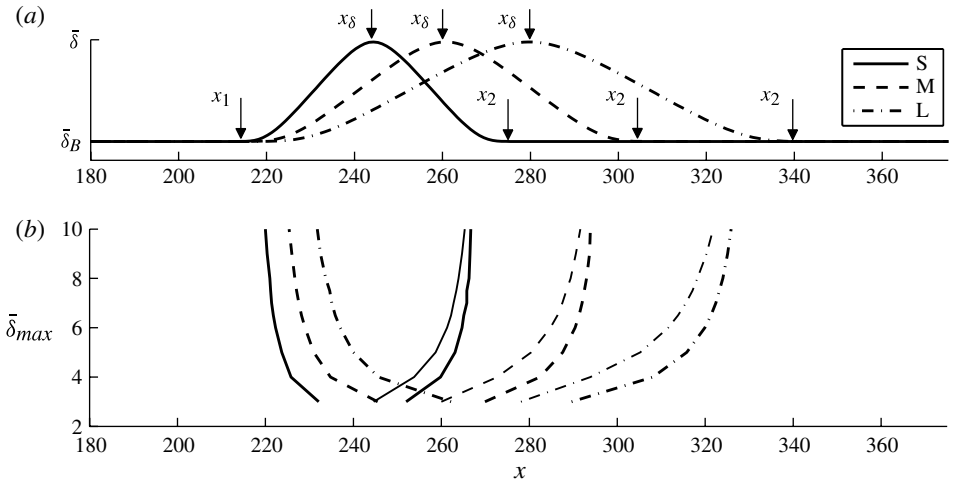


FIGURE 1. Laminar separation bubble models corresponding to cases S, M and L. (*a*) Transformed displacement thickness distribution $\bar{\delta}$. (*b*) Extent of the reversed flow region as a function of $\bar{\delta}_{max}$. Thick lines denote separation and reattachment lines and thin lines denote the location of the peak negative wall shear τ_{min}.

dimensionless velocities by $\bar{u}$ and $\bar{v}$. The chosen reference displacement thickness δ^*_{in} corresponds to $Re_{in} = 450$, and the respective inflow coordinate is $x = 152$. The same non-dimensionalization is used in the stability analyses in §§ 3 and 4.

An analytical displacement thickness distribution analogous to that prescribed by Carter (1975) is used for (2.4), in which $\bar{\delta}(x)$ starts at the Blasius value ($\bar{\delta}_B = 1.72078$) at the inflow boundary, is increased within a finite x-range until a maximum thickness $\bar{\delta}_{max}$ is attained, is then decreased until the Blasius solution is again recovered and is maintained constant until the outflow. The $\bar{\delta}(x)$ distribution is symmetric over x_δ, the location of $\bar{\delta}_{max}$, and the coordinates defining the start and end of the displacement thickness increase are respectively denoted as x_1 and x_2 ($x_\delta = (x_1 + x_2)/2$). Figure 1(*a*) shows the $\bar{\delta}$ distributions; the analytical definition of this function, which can be found in Rodríguez & Theofilis (2010*b*), is completely determined by x_1, x_2 and $\bar{\delta}_{max}$.

A series of base flows is computed. The coordinate $x_1 = 210$ is kept fixed and three different streamwise extents are considered: $x_2 = 264$, 290 and 320. For each extent, the value of $\bar{\delta}_{max}$ is varied from 3 to 10. In what follows the different base flows are designated by a letter corresponding to the deceleration extent: S for short, M for medium and L for long bubbles. Figures 1 and 2 summarize the characteristic parameters for the series of base flows considered. Figure 1(*b*) shows the location of the separation and reattachment points for each model bubble, as well as the location of the peak negative wall shear $\tau = f_{\eta\eta}$. In the cases where $\bar{\delta}_{max}$ is low, the wall shear distribution in the separated region is nearly symmetric, and the recirculation centre within the bubble is close to the centre of the deceleration region. As $\bar{\delta}_{max}$ is increased the peak wall shear is increased and displaced downstream, and therefore the recirculation centre moves downstream resulting in an asymmetric bubble. Figure 2(*a,b*) shows the peak values of the negative wall shear and the reversed flow, scaled with the inflow free-stream velocity $u_{rev} = u^*_{rev}/U^*_\infty$. It is noted that, using this formulation, the peak reversed flow cannot exceed $u_{rev} \approx 13\,\%$. This is because the

https://doi.org/10.1017/jfm.2013.504 Published online by Cambridge University Press

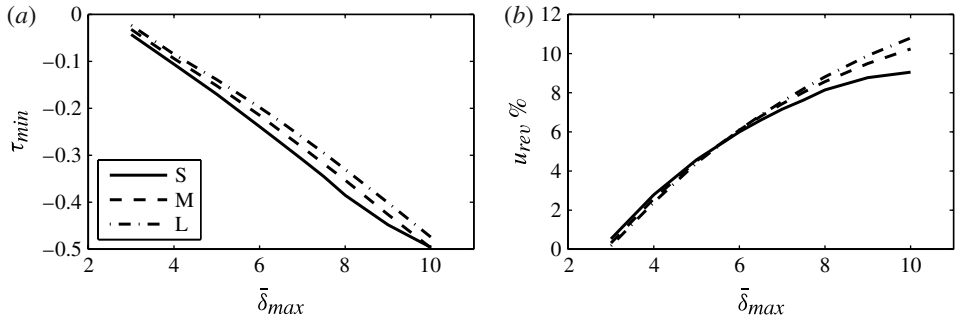


FIGURE 2. (*a*) Peak negative wall shear τ_{min} and (*b*) reversed flow u_{rev} %, as a function of $\bar{\delta}_{max}$.

peak reversed flow in Falkner–Skan profiles, which are asymptotic solutions of the present formulation, approximately matches this value (Schlichting 1979).

The present approach has been shown to recover realistic LSBs, in good agreement with those obtained by direct numerical simulations, when a physically sensible distribution of displacement thickness is imposed (Carter 1975; Rodríguez 2010).

3. Two-dimensional global oscillator

LSBs act as amplifiers of incoming disturbance waves, giving rise to amplifications that are orders of magnitude larger than those associated with zero-pressure-gradient or attached adverse-pressure-gradient boundary layers at the same Reynolds numbers. However, because this local instability is convective, it does not suffice to explain the onset of self-sustained oscillations of the bubble. In the case that the local analysis predicts a sufficiently large region of absolute instability, a global mechanism can exist leading to synchronized oscillations in the absence of external excitation. This possibility has been suggested in the past (Pauley *et al.* 1990; Allen & Riley 1995; Hammond & Redekopp 1998) to be responsible for the unsteadiness in separation bubbles. This section studies whether this is the case for the present series of bubbles.

3.1. *Locally parallel instability analysis*

The local analysis methodology considered here is explained in detail in Monkewitz, Huerre & Chomaz (1993) and Juniper *et al.* (2011). Only the main features are reproduced here. The locally parallel analysis assumes that the characteristic lengths of the instability waves and base flow in the streamwise direction are well-separated. This assumption leads to a succession of one-dimensional eigenvalue problems (EVPs) of the Orr–Sommerfeld class for the local instability of each slice X. The governing equations for a three-dimensional perturbation can be transformed, using Squire's transformation, into the governing equations for a two-dimensional perturbation at a lower Reynolds number. If the action of viscosity is purely stabilizing then it follows that, for a given Reynolds number, the three-dimensional wave is more stable than the two-dimensional wave. This is true for spatial, temporal, and spatio-temporal analyses. Consequently, only plane waves are considered in this analysis. The linearized Navier–Stokes equations (LNSE) are written as three partial differential equations (PDEs) in primitive variables, $\hat{\boldsymbol{q}} = (\hat{u}, \hat{v}, \hat{p})^{\mathrm{T}}$, and Fourier modes are introduced along the streamwise direction, leading to

$$\boldsymbol{q}'(x, y, t) = \hat{\boldsymbol{q}}(y) \exp[\mathrm{i}(kx - \omega t)]. \tag{3.1}$$

https://doi.org/10.1017/jfm.2013.504 Published online by Cambridge University Press

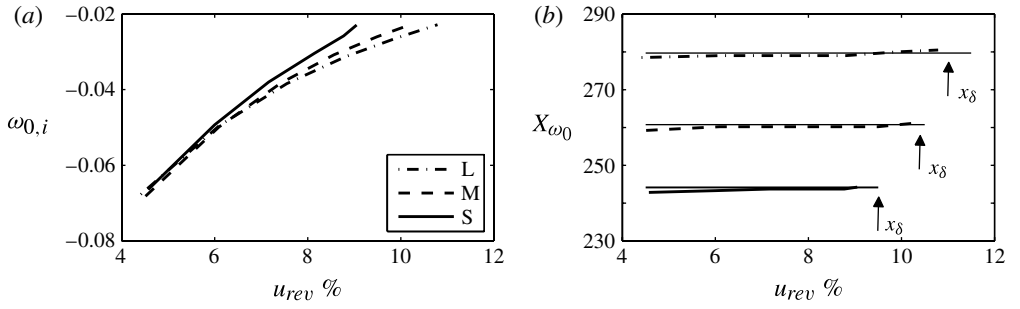


FIGURE 3. (*a*) Maximum absolute growth rate $\omega_{0,i}$ and (*b*) corresponding streamwise coordinate X_{ω_0}, as a function of the peak reversed flow u_{rev} %. The thin lines in (*b*) denote the location of the peak displacement thickness, $\bar{\delta}_{max}$.

This converts the PDEs into ordinary differential equations, which are discretized using Chebyshev polynomials in the y-direction, producing a generalized matrix EVP of the form

$$\boldsymbol{A}(k, \bar{\boldsymbol{q}}(X, y))\hat{\boldsymbol{q}}(y) = \omega \boldsymbol{B}(k, \bar{\boldsymbol{q}}(X, y))\hat{\boldsymbol{q}}(y). \tag{3.2}$$

At each slice of the flow, pairs of (ω, k) are found that satisfy both (3.2) and the additional criterion that $\mathrm{d}\omega/\mathrm{d}k = 0$. These pairs are labelled the absolute frequency and absolute wavenumber, $(\omega_0(X), k_0(X))$. The complex frequency of the linear oscillator mode, ω_g, is given by the saddle point of $\omega_0(X)$ in the complex-X-plane. If there is no absolute instability anywhere (i.e. $\omega_{0,i} < 0$ for every X) then the oscillator mode is stable ($\omega_{g,i} < 0$) and therefore cannot cause self-sustained oscillations.

3.2. *Results of locally parallel analysis*

Figure 3(*a,b*) shows the maximum absolute growth rate $\omega_{0,i}$ and the streamwise location X_{ω_0} where it is attained. The least stable region corresponds in all cases to the vicinity of the maximum displacement thickness of the bubble, where the inflection point is furthest from the wall. This finding is in line with the stability analyses of Rist & Maucher (2002), and suggests that the peak displacement thickness $\bar{\delta}_{max}$ is the most representative quantity in the local analysis. This contrasts with analyses of unbounded mixing layers (Huerre & Monkewitz 1985) for which the peak reversed flow was shown to govern the instability. In the present bubbles, the peak reversed flow occurs downstream of the peak displacement thickness.

No regions of absolute instability were found for any of the model bubbles, and consequently the oscillator mechanism cannot lead to unsteadiness in the absence of external excitation. The trends observed in figure 3(*a*) suggest that a base bubble with a peak reversed flow much larger than $u_{rev} = 12\,\%$ would be required for the onset of absolute instability.

4. Global centrifugal instability

Steady two-dimensional separation bubbles can become unstable to three-dimensional perturbations if the recirculation is strong enough, in terms of peak reversed flow or minimum wall shear. By means of the PDE-based global instability analysis, this instability is recovered as a single discrete eigenmode. The existence of this eigenmode and its perturbation structure have been documented for different flow

https://doi.org/10.1017/jfm.2013.504 Published online by Cambridge University Press

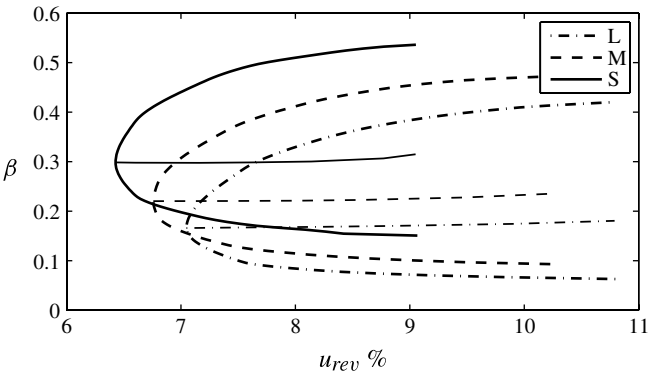


FIGURE 4. Neutral curves (thick lines) for the steady three-dimensional global mode, depending on the spanwise wavenumber β and the peak reversed flow u_{rev} %, for the three deceleration lengths. The thin lines correspond to the most amplified spanwise wavenumber.

configurations featuring two-dimensional recirculation bubbles (Theofilis *et al.* 2000; Barkley *et al.* 2002; Gallaire *et al.* 2007; Marquet *et al.* 2008; Kitsios *et al.* 2009). This eigenmode corresponds to a centrifugal instability, which causes a steady three-dimensionalization of the recirculation region. Due to the structural instability of the two-dimensional base flow topology, the perturbed flow on account of the centrifugal instability exhibits a different topological description regardless of the smallness of the perturbation amplitude, as discussed by Rodríguez & Theofilis (2010*b*).

4.1. *Global instability analysis*

Following from the two-dimensionality of the base flow and using separation of variables, modal linear perturbations can be written, without loss of generality, as

$$\boldsymbol{q}'(x, y, z, t) = \hat{\boldsymbol{q}}(x, y) \exp[\mathrm{i}(\beta z - \omega t)]. \tag{4.1}$$

Here β is a wavenumber in the spanwise direction defining a periodicity length $\lambda_z = 2\pi/\beta$. Introducing this decomposition into the LNSE, one arrives at a PDE-based eigenvalue problem that, after discretization, takes the form

$$\boldsymbol{A}(\beta, \bar{\boldsymbol{q}})\hat{\boldsymbol{q}}(x, y) = \omega \boldsymbol{B}\hat{\boldsymbol{q}}(x, y). \tag{4.2}$$

Stability analyses based on the solution of PDE-based EVPs are often limited by the large size of the discretized matrices $\boldsymbol{A}$ and $\boldsymbol{B}$. A shift-and-invert implementation of the Arnoldi algorithm (Theofilis 2003, 2011) is used here to recover efficiently a reduced window of the eigenspectrum. A novel algorithm that combines high-order finite differences with sparse algebra (Amestoy *et al.* 2001) is employed, drastically reducing the computational resources required by the spectral collocation and distributed-memory dense algebra solutions employed in our previous studies (Rodríguez & Theofilis 2009, 2010*b*; Juniper *et al.* 2011). The improved efficiency of the new algorithm (Gennaro *et al.* 2013) enables the large parametric study presented next.

4.2. *Results of the global analysis*

The neutral curves corresponding to the centrifugal instability eigenmode for the three deceleration lengths (S, M and L) are shown in figure 4, as a function of the spanwise

https://doi.org/10.1017/jfm.2013.504 Published online by Cambridge University Press

wavenumber and the peak reversed flow. Consistent with results in the literature, the eigenmode is unstable for a bounded range of β values, and attains the maximum amplification for a finite spanwise wavenumber. Qualitatively identical behaviour is found for the three streamwise extents, with the dominant β (shown by the thin lines) decreasing as the deceleration length increases but being nearly independent of the peak recirculation. The critical peak recirculation, i.e. the value of the reversed flow for which the eigenmode becomes unstable, is well below $u_{rev} = 10\,\%$ in all cases.

5. Conclusions

The linear global instability of a series of model LSBs has been analysed with the aim of determining the possible routes to three-dimensionalization and unsteadiness of nominally two-dimensional base states in the absence of external excitation. The two main global mechanisms found in the literature have been addressed: a global oscillator due to localized regions of absolute instability of K–H waves, and a centrifugal instability leading to steady three-dimensionalization of the base LSB. The main objective of the analyses is the determination of the primary instability, i.e. which mechanism becomes active first as the strength of the recirculation region increases. Both instabilities are of inviscid nature, and the Reynolds number is expected to have a very limited effect as long as it is high enough. In line with other studies in the literature, the peak reversed flow u_{rev} was used here as a measure of the bubble strength, but it was found not to be the most representative parameter either for the locally parallel analysis, for which the maximum displacement thickness was found to be more adequate, or for the centrifugal instability for which a representative parameter is still to be determined.

The present results show that the instability of planar waves is only convective for the model LSBs considered, in line with the relatively low $u_{rev} < 12\,\%$ compared to the $u_{rev} \approx 20\,\%$ threshold values found in the literature for the onset of absolute instability. On the other hand, the three-dimensional, centrifugal mechanism becomes linearly unstable about $u_{rev} \approx 7\,\%$, and the trends observed in the growth rates (figure 3*a*) do not suggest that the oscillator mechanism would become unstable or dominant if longer bubbles were considered, because it is governed by the velocity profile at the location of the peak displacement thickness. The conclusion is that the primary instability acting on flat-plate LSBs in the absence of external forcing gives rise to a steady three-dimensionalization of the bubble rather than to two-dimensional vortex shedding. Independent theoretical (Barkley *et al.* 2002; Gallaire *et al.* 2007; Marquet *et al.* 2008) and experimental studies (Beaudoin *et al.* 2004; Passaggia, Leweke & Ehrenstein 2012) for related separated flows show the same bifurcation path. Secondary instabilities as a result of the topological changes resulting from the temporal amplification of the centrifugal mode (Theofilis *et al.* 2000; Rodríguez & Theofilis 2010*b*) are then a possible path to unsteadiness that is currently being studied. The completion of this research is expected to explain the large disagreement in the peak reversed flow required for the onset of unsteadiness in two-dimensional ($u_{rev} \approx 20\,\%$, e.g. Fasel & Postl 2004) and three-dimensional ($u_{rev} \leqslant 10\,\%$, e.g. Alam & Sandham 2000) unforced DNS.

Similarly, a complete understanding of the transition process initiated by the three-dimensional instability on unforced bubbles may shed light on the physical origin of bursting. Bursting is associated with experimental conditions in which external disturbances, though with small initial amplitudes, are present and the amplifier character of LSBs dominates. It is possible, however, that the spanwise modulation

https://doi.org/10.1017/jfm.2013.504 Published online by Cambridge University Press

caused by the centrifugal instability of the mean separation bubble alters significantly the manner in which the amplifier behaviour of the bubble is manifested, determining the qualitative (short or long) character of the bubble.

Acknowledgements

Discussions with Professors V. Theofilis and O. N. Ramesh are kindly acknowledged. D.R. acknowledges funding from the European Union Marie Curie – COFUND programme. The work of E.M.G. is supported by CNPq/Brazil.

References

ALAM, M. & SANDHAM, N. D. 2000 Direct numerical simulation of 'short' laminar separation bubbles with turbulent reattachment. *J. Fluid Mech.* **410**, 1–28.

ALLEN, T. & RILEY, N. 1995 Absolute and convective instabilities in separation bubbles. *Aeronaut. J.* **99**, 439–448.

AMESTOY, P. R., DUFF, I. S., L'EXCELLENT, J.-Y. & KOSTER, J. 2001 A fully asynchronous multifrontal solver using distributed dynamic scheduling. *SIAM J. Matrix Anal. Applics.* **23** (1), 15–41.

BARKLEY, D., GOMES, M. G. M. & HENDERSON, R. D. 2002 Three-dimensional instability in a flow over a backward-facing step. *J. Fluid Mech.* **473**, 167–190.

BEAUDOIN, J., CADOT, O., AIDER, J. & WESFREID, J. 2004 Three-dimensional stationary flow over a backward-facing step. *Eur. J. Mech. (*B*/Fluids*) **23**, 147–155.

CARTER, J. 1975 Inverse solutions for laminar boundary-layer flows with separation and reattachment. *NASA Tech. Rep.* TR R-447.

CEBECI, T. & COUSTEIX, J. 2005 *Modelling and Computation of Boundary-Layer Flows – Solutions Manual and Computer Programs*. Springer.

DALLMANN, U. & SCHEWE, G. 1987 On topological changes of separating flow structures at transition Reynolds numbers. In *16th Fluid Dynamics, Plasma Dynamics and Lasers Conference, Honolulu, HI. AIAA Paper* 87-1266.

DIWAN, S. S. 2009 Dynamics of early stages of transition in a laminar separation bubble. PhD thesis, Indian Institute of Science, Bangalore, India.

DIWAN, S., CHETAN, S. & RAMESH, O. 2006 On the bursting criterion for laminar separation bubbles. In *Sixth IUTAM Symposium on Laminar–Turbulent Transition* (ed. R. Govindarajan), pp. 401–407. Springer.

DIWAN, S. & RAMESH, O. 2009 On the origin of the inflectional instability of a laminar separation bubble. *J. Fluid Mech.* **629**, 263–298.

DIWAN, S. & RAMESH, O. 2012 Relevance of local parallel theory to the linear stability of laminar separation bubbles. *J. Fluid Mech.* **698**, 468–478.

DOVGAL, A., KOZLOV, V. & MICHALKE, A. 1994 Laminar boundary layer separation: instability and associated phenomena. *Prog. Aero. Sci.* **3**, 61–94.

FASEL, H. F. & POSTL, D. 2004 Interaction of separation and transition of three-dimensional development in boundary layer transition. In *Sixth IUTAM Symposium on Laminar-Turbulent Transition* (ed. R. Govindarajan), pp. 71–88. Springer.

GALLAIRE, F., MARQUILLIE, M. & EHRENSTEIN, U. 2007 Three-dimensional transverse instabilities in detached boundary layers. *J. Fluid Mech.* **571**, 221–233.

GASTER, M. 1967 The structure and behaviour of separation bubbles. *NPL R & M* 3595.

GASTER, M. 2004 Laminar separation bubbles. In *Sixth IUTAM Symposium on Laminar-Turbulent Transition* (ed. R. Govindarajan)), pp. 1–13. Springer.

GAULT, D. 1949 Boundary-layer and stalling characteristics of the NACA 63-009 airfoil section. *NACA TN* 1894.

GENNARO, E. M., RODRÍGUEZ, D., MEDEIROS, M. A. F. & THEOFILIS, V. 2013 Sparse techniques in global flow instability with application to compressible leading-edge flow. *AIAA J.* **51** (9), 2295–2303.

https://doi.org/10.1017/jfm.2013.504 Published online by Cambridge University Press

GRUBER, K., BESTEK, H. & FASEL, H. 1987 Interaction between a Tollmien–Schlichting wave and a laminar separation bubble. *AIAA Paper* 87-1256.

HAMMOND, D. & REDEKOPP, L. 1998 Local and global instability properties of separation bubbles. *Eur. J. Mech. (*B*/Fluids*) **17**, 145–164.

HUERRE, P. & MONKEWITZ, P. 1985 Absolute and convective instabilities in free shear layers. *J. Fluid Mech.* **159**, 151–168.

HUERRE, P. & MONKEWITZ, P. 1990 Local and global instabilities in spatially developing flows. *Annu. Rev. Fluid Mech.* **22**, 473–537.

JUNIPER, M. P., TAMMISOLA, O. & LUNDELL, F. 2011 The local and global stability of confined planar wakes at intermediate Reynolds number. *J. Fluid Mech.* **686**, 218–238.

KITSIOS, V., RODRÍGUEZ, D., THEOFILIS, V., OOI, A. & SORIA, J. 2009 Biglobal stability analysis in curvilinear coordinates of massively separated lifting bodies. *J. Comput. Phys.* **228**, 7181–7196.

MARQUET, O., SIPP, D., CHOMAZ, J. & JACQUIN, L. 2008 Amplifier and resonator dynamics of a low-Reynolds-number recirculation bubble in a global framework. *J. Fluid Mech.* **605**, 429–443.

MARXEN, O. & HENNINGSON, D. S. 2011 The effect of small-amplitude convective disturbances on the size and bursting of a laminar separation bubble. *J. Fluid Mech.* **671**, 1–33.

MARXEN, O., LANG, M. & RIST, U. 2012 Discrete linear local eigenmodes in a separating laminar boundary layer. *J. Fluid Mech.* **711**, 1–26.

MCCULLOUGH, G. & GAULT, D. 1951 Examples of three representative types of airfoil-section stall at low speed. *NACA TN* 2502.

MONKEWITZ, P., HUERRE, P. & CHOMAZ, J. M. 1993 Global linear stability analysis of weakly non-parallel shear flows. *J. Fluid Mech.* **251**, 1–20.

PASSAGGIA, P.-Y., LEWEKE, T. & EHRENSTEIN, U. 2012 Transverse instability and low-frequency flapping in incompressible separated boundary layer flows: an experimental study. *J. Fluid Mech.* **703**, 363–373.

PAULEY, L., MOIN, P. & REYNOLDS, W. 1990 The structure of two-dimensional separation. *J. Fluid Mech.* **220**, 397–411.

RIST, U. & MAUCHER, U. 1994 Direct numerical simulation of 2-d and 3-d instability waves in a laminar separation bubble. In *AGARD-CP-551 Application of Direct and Large Eddy Simulation to Transition and Turbulence* (ed. B. Cantwell), pp. 34-1–34-7.

RIST, U. & MAUCHER, U. 2002 Investigations of time-growing instabilities in laminar separation bubbles. *Eur. J. Mech. (*B*/Fluids)* **21**, 495–509.

RODRÍGUEZ, D. 2010 Global stability of laminar separation bubbles. PhD thesis, Universidad Politecnica de Madrid.

RODRÍGUEZ, D. & THEOFILIS, V. 2009 Massively parallel numerical solution of the biglobal linear instability eigenvalue problem using dense linear algebra. *AIAA J.* **47** (10), 2449–2459.

RODRÍGUEZ, D. & THEOFILIS, V. 2010*a* On the birth of stall cells on airfoils. *Theor. Comput. Fluid Dyn.* **25**, 105–117.

RODRÍGUEZ, D. & THEOFILIS, V. 2010*b* Structural changes of laminar separation bubbles induced by global linear instability. *J. Fluid Mech.* **655**, 280–305.

SCHLICHTING, H. 1979 *Boundary Layer Theory*, 7th edn. McGraw-Hill.

THEOFILIS, V. 2003 Advances in global linear instability analysis of nonparallel and three-dimensional flows. *Prog. Aero. Sci.* **39**, 249–315.

THEOFILIS, V. 2011 Global linear stability. *Annu. Rev. Fluid Mech.* **43**, 319–352.

THEOFILIS, V., HEIN, S. & DALLMANN, U. 2000 On the origins of unsteadiness and three-dimensionality in a laminar separation bubble. *Phil. Trans. R. Soc. Lond.* A **358**, 3229–3246.

WATMUFF, J. H. 1999 Evolution of a wave packet into vortex loops in a laminar separation bubble. *J. Fluid Mech.* **397**, 119–169.

YON, S. & KATZ, J. 1998 Study of the unsteady flow features on a stalled wing. *AIAA J.* **36** (3), 305–312.

ZAMAN, K., MCKINZIE, D. & RUMSEY, C. 1989 A natural low-frequency oscillation of the flow over an airfoil near stalling conditions. *J. Fluid Mech.* **202**, 403–442.

https://doi.org/10.1017/jfm.2013.504 Published online by Cambridge University Press